



## Martensitic phase transformation of Cu-Zn-Al alloy, induced by cold rolling deformation

S. Natali, V. Volpe, L. Zortea

*“Sapienza” University of Rome, Dip.I.C.M.A., Via Eudossiana 18, 00184, Rome, Italy*  
stefano.natali@uniroma1.it

V. Di Cocco, F. Iacoviello

*University of Cassino, DICeM, via G. Di Biasio 43, 03043 Cassino (FR), Italy*

---

**ABSTRACT.** The purpose of this paper is to study the phase transformation induced by the cold rolling of a Cu-Zn-Al alloy fabricated in our laboratories. Flat specimens were made from the alloy. They were subsequently heat treated at 850°C/20 min, quenched in water at 100°C, treated at 320°C/30 min, quenched in water at 100°C, cooled in air up to room temperature.

To correlate the microstructure variations with the entity of the imposed deformation, the samples were cold rolled selectively (each 2.5%) up to 15% of deformation. On each cold rolled sample, the microstructures were investigated by LOM and XRD. The deformation has contributed to  $\beta_3$  ( $L_{21}$ ) ordering of the structure and to occur the martensitic transformation. The martensite obtained is the M18R type.

This result shows that the parameter which most influences the type of obtainable martensite is determined by the order of the parent phase. During testing it was found that the martensite nucleates in appreciable quantities even at a level of deformation of 2.5% of the specimen. An increase of the martensite up to a deformation of 15% was observed. It has not been possible to continue beyond this level of deformation, due to the presence of transgranular cracks.

**SOMMARIO.** Nel presente lavoro è stato affrontato lo studio della trasformazione di fase indotta dalla laminazione a freddo su una lega Cu-Zn-Al prodotta in laboratorio. Dalla lega sono stati realizzati alcuni provini piatti successivamente trattati termicamente a 850°C/20 min, temprati in acqua a 100°C, trattati a 320°C/30 min, temprati in acqua a 100°C, raffreddati in aria fino a T ambiente.

Per correlare le variazioni della microstruttura con l'entità delle deformazioni imposte, i campioni sono stati laminati a freddo selettivamente (ogni 2.5%) fino al 15 % di deformazione. Su ciascun campione deformato sono state analizzate le strutture tramite osservazioni al microscopio ottico e con tecniche di diffrazione di raggi X. La deformazione ha contribuito da un lato all'ordinamento della struttura  $\beta_3$  ( $L_{21}$ ) e dall'altro a far avvenire la trasformazione martensitica. La martensite ottenuta è del tipo M18R.

Tale risultato dimostra che il parametro che maggiormente influenza la tipologia di martensite ottenibile è determinato dall'ordine delle fase genitrice. Durante la sperimentazione si è potuto constatare che già ad un livello di deformazione del 2,5% la martensite nuclea in apprezzabili quantità. Per livelli di deformazione crescente si è osservato un aumento della martensite fino ad una deformazione del 15%, oltre tale livello di deformazione non è stato possibile proseguire a causa della presenza di cricche transgranulari.

**KEYWORDS.** Shape Memory Alloys; Stress-induced martensitic transformation; X-Ray Diffraction.

---



## INTRODUCTION

The Shape Memory Alloys (SMA) of the ternary system Cu-Zn-Al have recently received the attention of researchers for their low cost and for the variety of interesting mechanical and thermal properties as the pseudoelasticity (PE) and the shape memory effect (SME). These properties are directly associated with the thermoelastic martensitic transformation [1]. Such alloys solidify in a body-centered cubic structure ( $A_2$ ), disordered, called  $\beta$  phase which is stable at high temperature, and during cooling undergo two order types. The first ( $B_2$ ) occurs at a temperature of about 550°C and it is a super lattice of the CsCl type, also referred as  $\beta_2$  [2]. The second ( $L_{21}$ ), induced by further cooling, can be observed already at a temperature of about 320°C and it is a super lattice of the type  $Cu_2MnAl$  also referred as  $\beta_3$  [3]. Many experimental results and theoretical analysis [4,5] have shown that the characteristics of martensitic transformations (9R, 18R) are derived and related to the properties that the parent ordered phase ( $B_2$ ,  $L_{21}$ ) owns during quenching. The martensitic transformation can be induced by the rapid cooling of the alloy, below the start transformation temperature ( $M_s$ ), and also by the application of an external stress, deforming the structure at temperatures higher than  $M_s$ . Although there are many experimental studies carried out to understand the temperature effects in SMA alloys used in several devices [6], there is a lack of literature which deepens the knowledge of stress effects and of the behavior under stress of polycrystalline  $\beta$  Cu-Zn-Al alloys. The aim of this preliminary study is to investigate and describe, using optical microscopy and X-ray diffraction techniques, the structural change induced in a cold rolled Cu-Zn-Al.

## EXPERIMENTAL DETAILS

Experiments were performed with an alloy with a composition within the  $\beta$  area of the diagram. The compositions usable to fit in the  $\beta$  area of the diagram are various and can be obtained by varying both the zinc and the aluminum content.

In this work we have used a Cu-Zn-Al alloy with the 4.8 wt% of aluminum in order to make it easily cold rollable. The alloy was fabricated using an induction furnace for performing centrifugal castings and under inert atmosphere (argon). A yttria crucible filled with a binary commercial brass (CuZn30) and appropriate additions of Cu and Al was used to melt the metal. The casting was carried out in a graphite mould and it was made a prismatic ingot with square base, Fig.1a, size (66x12x9) mm. The cooling was performed with quenching in water at  $T = 25^\circ\text{C}$ . Tab. 1 shows the composition of the alloy obtained.

Weight %			Atomic %			e/a
Cu	Zn	Al	Cu	Zn	Al	
71.29	23.89	4.80	67.36	21.94	10.69	1.4331

Table 1: Chemical composition of alloy and electron-atom (e/a) ratio.



Figure 1a: As cast ingot

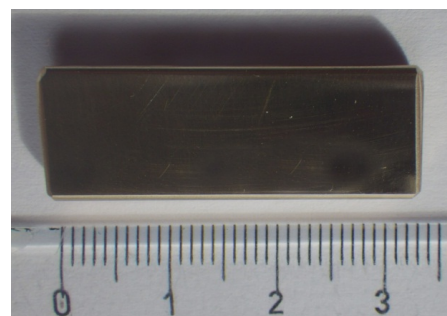


Figure 1b: Sample before the cold rolling

Six samples (33 mm x 11.5 mm x 3.4 mm) were obtained from the fabricated ingot by cutting the cross and the longitudinal section, to be used for both lamination and microstructural observations. All the samples were grinded with silicon carbide abrasive papers and then lapped using 1-micron alumina to limit the occurrence, during the rolling, of possible cracks. Fig.1b shows one of the samples before lamination.



Finally all the samples were treated at 850°C, existence range of the  $\beta$  phase (austenite), for 20 minutes and subsequently quenched in water at 100°C. After quenching, the samples were treated again at 320°C for 30 minutes, then cooled in water at 100°C for 30 minutes and then cooled in air.

The permanence at the temperature of 850°C determines the homogenization of the  $\beta$  phase, while the one at 320°C promotes the long range order [8], in fact the  $\beta$  phase in these alloys presents two types of order ( $B_2$  and  $L_{21}$ ) that are determined at temperatures that depend on the chemical composition [9,10].

The operations of cutting and mechanical polishing were performed before the thermal treatment of the  $\beta$  phase stabilization. Furthermore the lapping process has been executed even after the heat treatment in order to remove the surface oxide layer that is formed by the permanence in the oven. The samples were cold rolled by performing all the operations at a temperature of  $T = 25^\circ\text{C}$ . Contrary to what occurs in hot rolling, in this case, each step at the rolling mill was not interrupted by thermal treatments of annealing to not alter the specimen structure. In fact the aim of the experimentation is to correlate the effects of the lamination with the nucleation and the growth of martensite induced only by plastic deformation. During the tests each sample was subjected to a deformation of 2.5% up to, with subsequent steps, the maximum deformation of 15%. Each step has been documented by optical microscopy and X-ray diffraction.

The average percentage of cold working  $L\%$ , has been defined as:

$$L\% = \frac{b_0 - b_f}{b_0} \cdot 100$$

Where:  $L\%$  = deformation rate

$b_f$  = final thickness of the rolled sample after rolling

$b_0$  = initial thickness of the sample before rolling

For each step of deformation of 2.5% it was necessary to reduce the initial thickness of a quantity equal to 0.085 mm. Tab. 2 reports the data of the subsequent laminations for a representative specimen of the entire group of samples:

Deformation Set	$h_0$ (mm)	$h_f$ (mm)
2.5%	3.4	3.315
5%	3.315	3.25
7.5%	3.25	3.145
10%	3.145	3.06
12.5%	3.06	2.975
15%	2.975	2.89

Table 2: Data of the subsequent laminations.

For the microstructural investigation, the samples were subjected to chemical etching by immersion at room temperature, for 30 seconds, in a solution consisting of 3 g of ferric chloride ( $\text{FeCl}_3$ ), 10  $\text{cm}^3$  of hydrochloric acid (HCl) and 90  $\text{cm}^3$  of ethanol ( $\text{C}_2\text{H}_5\text{OH}$ ).

XRD measurements were carried out by using a Philips X-PERT PRO diffractometer equipped with vertical Bragg-Brentano powder goniometer. A step-scan mode was used in the  $2\theta$  range from  $25^\circ$  to  $90^\circ$  with a step width of  $0.02^\circ$  and a counting time of 3 s per step, and receiving slit 0.02 mm. The employed radiation was monochromated  $\text{Cu K}\alpha$  (40kV – 40 mA). The calculation of theoretical diffractograms and the generation of structure models were performed using the Powder Cell software [11].

## RESULTS AND DISCUSSION

After the heat treatment of ordering ( $320^\circ\text{C}/30'$ ), a metallographic analysis was performed with an optical microscope. The LOM micrographs show the typical structure of the  $\beta$  phase characterized by grains uniformly distributed, regular and equiaxed (Fig. 2a). The X-ray diffraction analysis has confirmed that the performed thermal treatment was able to give an ordering to the specimens. Indeed, as seen from the diffractogram in Fig.2b relative



to one of the treated samples, the structure is the  $\beta_3$  ( $L_{21}$ ) type, the peaks (200), (220) and (422) are typical of this ordered phase, that has a lattice parameter of the cell (a) equal to 5.8707 Å.



Figure 2a: Microstructure after thermal treatment.

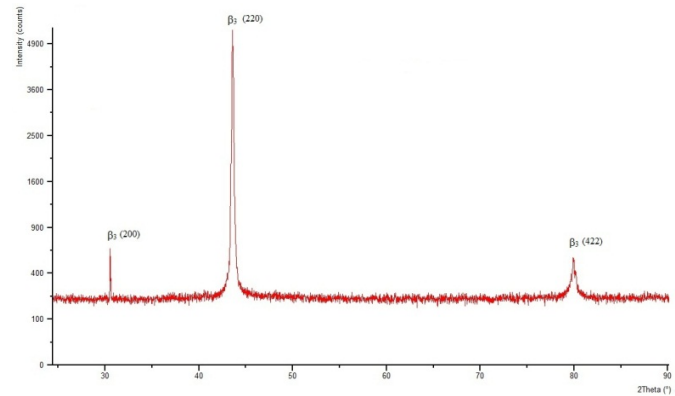


Figure 2b: Diffractogram of a thermally treated specimen.

The effects of the deformation on the structure of the rolled samples are visible in Fig.3: in which is shown the comparison between the diffractogram of a not deformed sample with one deformed up to 2.5%.

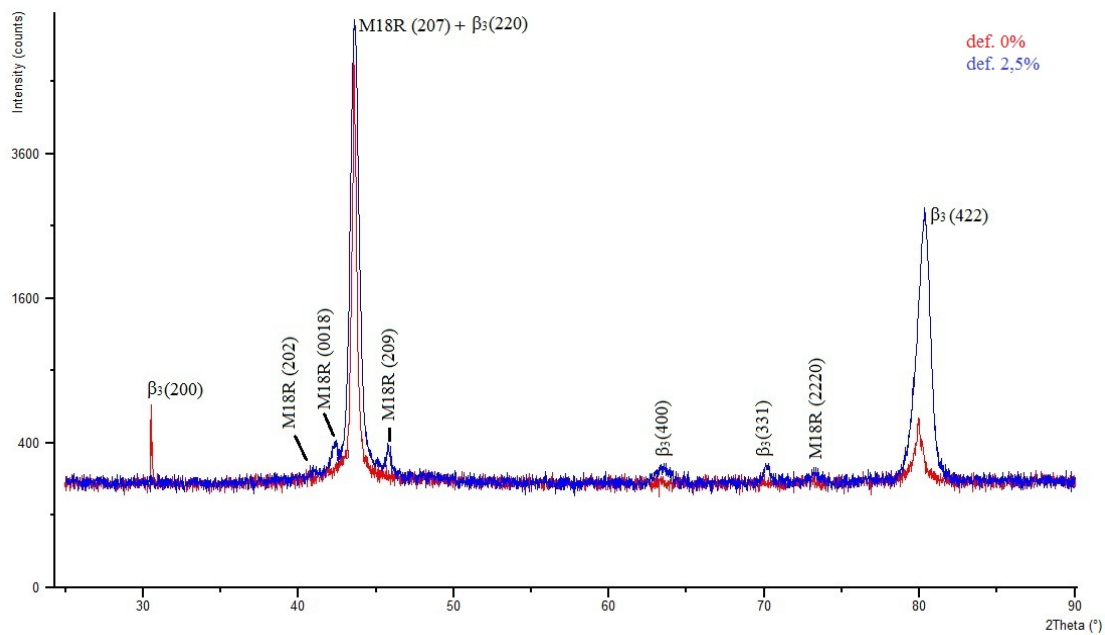


Figure 3: Comparison between the diffractogram of a not deformed sample with one deformed up to 2.5%.

It can be observed that compared to the non-deformed sample, in the one deformed by 2.5% there is the rise of new peaks, namely the (400) and (331), and the disappearance of the peak (200) all belonging to the ordered  $\beta_3$  phase.

Furthermore, we can notice two phenomena:

- A rightward shift of the two peaks of such phase, (220) and (422), compared to the position taken in the diffractogram performed before the mechanical treatment. This shift indicates a compaction of the structure (ccc) of the ordered phase; the lattice parameter (a) that characterizes the cubic structure in fact, decreases from a value of 5.8707 Å to 5.8550 Å thus indicating compaction of the cell.

- The presence of new peaks belonging to a structure of the M18R type [12].

The stress imposed by the rolling has therefore had the effect to contribute to ordering the structure and to cause the martensite transformation. The lattice parameters of the M18R martensite are reported in Tab. 3.



Martensite	<i>a</i>	<i>b</i>	<i>c</i>	$\beta$
M18R	4.486	5.339	38.432	89.45

Table 3: M18R martensite lattice parameters obtained by plastic deformation.

The typical peaks of the M18R martensitic structure are related to the reflection planes characterized by Miller indexes (202) (0018) (207) (209) and (2220) [13]. As it can be observed from the diffractogram the peak (207) of martensite creates a constructive interference with the peak (220) relative to the  $\beta_3$  determining the impossibility to associate the respective intensities to the relative phase. This phenomenon of constructive interference determines the classification of the (207) plane as a martensite plane of habitus.

The nucleation of martensite is also demonstrated by the metallographic analysis carried out by means of light microscope. Fig. 4 shows the presence of small laths of martensite already formed, the needle-like lines are cross sections of two-dimensional martensite plates.

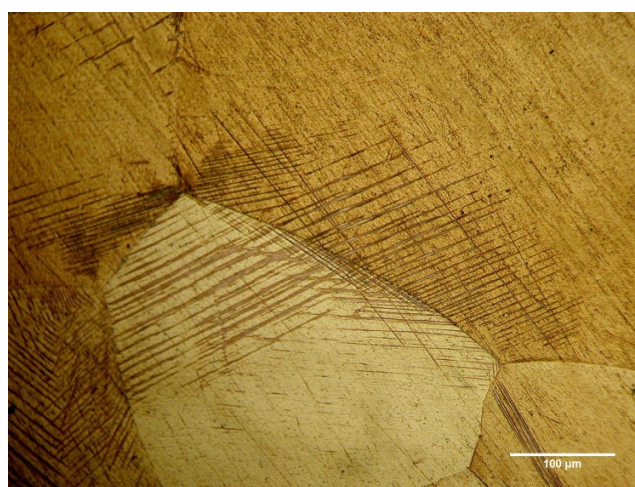


Figure 4: 200X LOM micrograph of a sample deformed up to 2.5%.

The subsequent laminations lead to an increase of the plastic deformation and they cause a growth of the martensitic structure. Fig. 5 shows the diffractogram relating to the state of deformation of 7.5%.

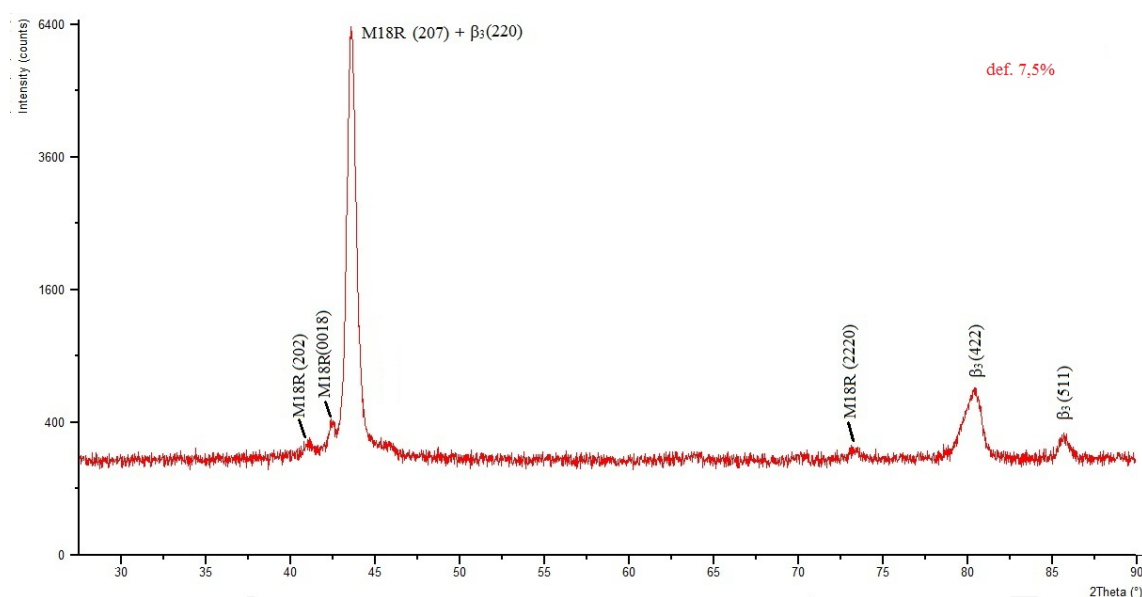


Figure 5: Diffractogram of a sample deformed up to 7.5%.





The increase of intensity of the martensite peaks (202) and (207) can be observed in this diffractogram; although for the latter there is the constructive interference of the martensite and of the  $\beta_3$  phase, it is reasonable to assume that its increase in intensity is due to the growth of martensite along the (207) plane. A confirmation of what it was hypothesized is given from an intensity decrease of the  $\beta_3$  phase peak (422) and the disappearance of those with Miller indexes (400) and (331), balanced in part by the rise of the new peak (511). Metallographic analysis shows that the sample has a higher amount of martensite, characterized by thin laths and finely distributed within the grains. In Fig. 6a it can be observed how the formation of martensite within the grains is strongly dependent on their crystallographic orientation [14], while twinning planes along which the martensite is generated are clearly visible in Fig. 6b. This kind of martensite appears in parallel bands alternately containing a different variant.



Figure 6a: 100X LOM micrograph of a sample deformed up to 7.5%: strips of variously oriented martensite.

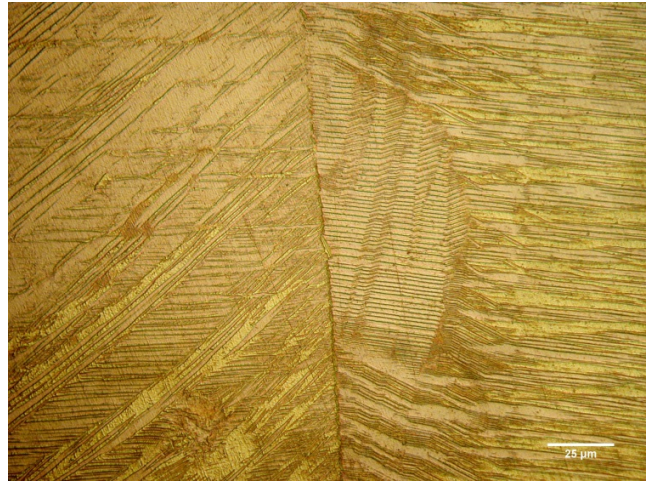


Figure 6b: 500X LOM micrograph of a sample deformed up to 7.5%: twinning plans.

Continuing with the rolling up to a plastic deformation of 12.5%, it is observed that the process increases continuously the martensite, in fact, it triggers the nucleation of the same along another plane, i.e. the plane with Miller indexes (209). Moreover, as can be seen from the diffractogram in Fig. 7, relative to this state of deformation, the peaks (202) (0018) have increased their intensity.

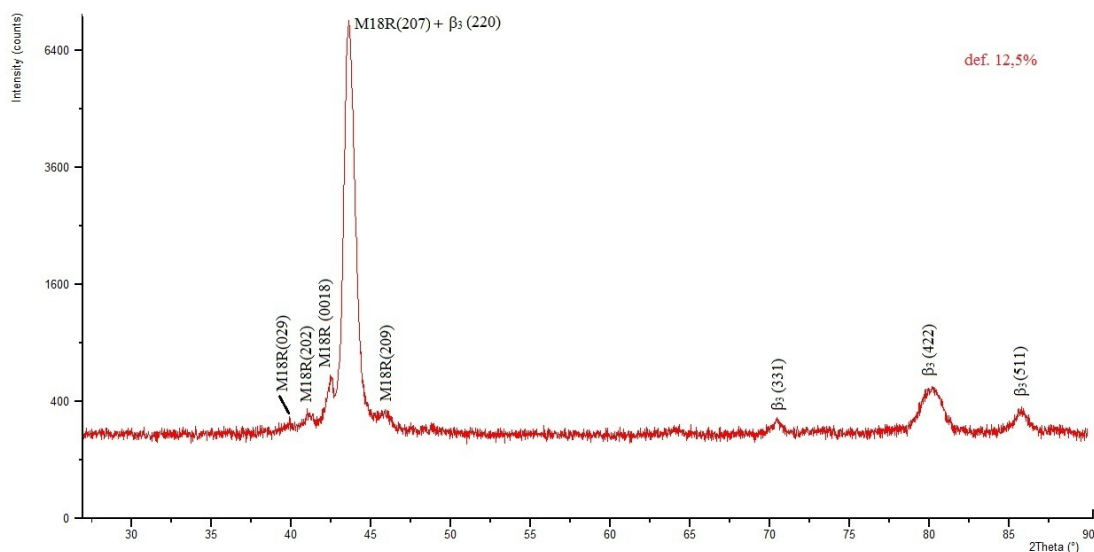


Fig. 7 Diffractogram of a sample deformed up to 12.5%



The rolling process has also influenced the martensite structure further deforming the M18R cell; the parameter relative to the  $\beta$  angle of inclination of the unit cell, in fact, passes from a value of  $89.45^\circ$  to  $89.75^\circ$ , showing a further distortion of the structure.

For the  $\beta_3$  phase a decrease of the peak (422) is observed. Fig. 8 shows micrographs of samples deformed up to 12.5%; the images show that the morphology of the obtained martensite is the typical one reported in the literature [14,15], consisting of thin laths and finely distributed that develop on different orientations. The martensitic transformation obtained is the "twinned" type, alias obtained by an arrangement of the crystal lattice in the parent phase.

This alloy responds to stresses induced by simply changing the orientation of its crystal structure, thanks to the movement through twinning of two neighboring areas, so it will be deformed in this way as long as there is a stress state along the twinning planes.

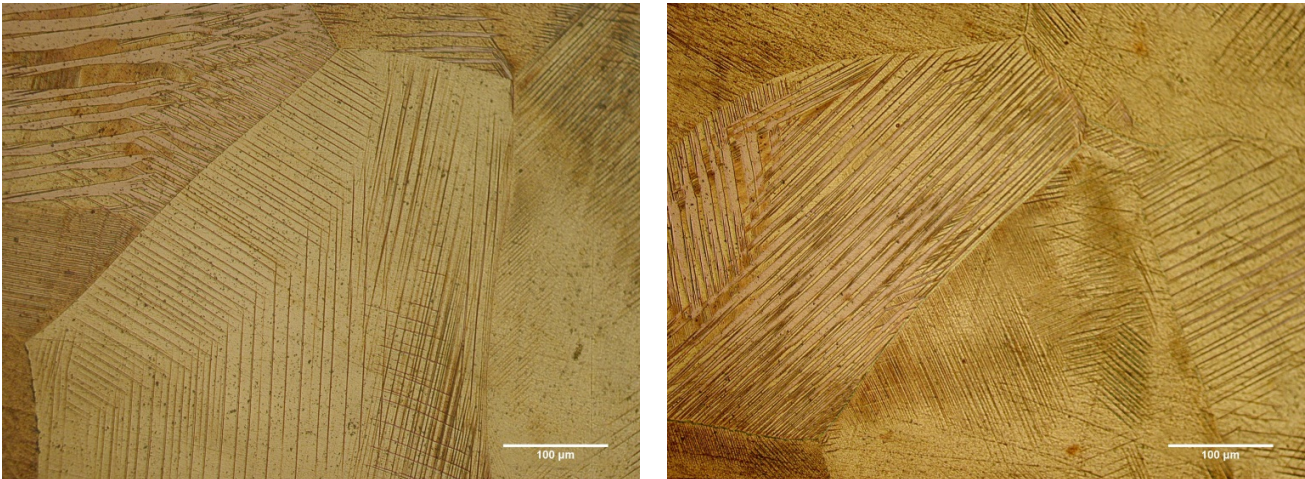


Figure 8: 200X LOM micrographs of a sample deformed up to 12.5%

The diffractogram of Fig. 9 relative to the deformation of 15% shows an increase in intensity of the martensite peaks compared to the diffractograms of 7.5% and 12.5% deformation. It also shows a tendency to the stabilization of the same. An impossibility of increase of the fraction of martensite caused by the work hardening of the  $\beta_3$  phase is shown at this stage of deformation.

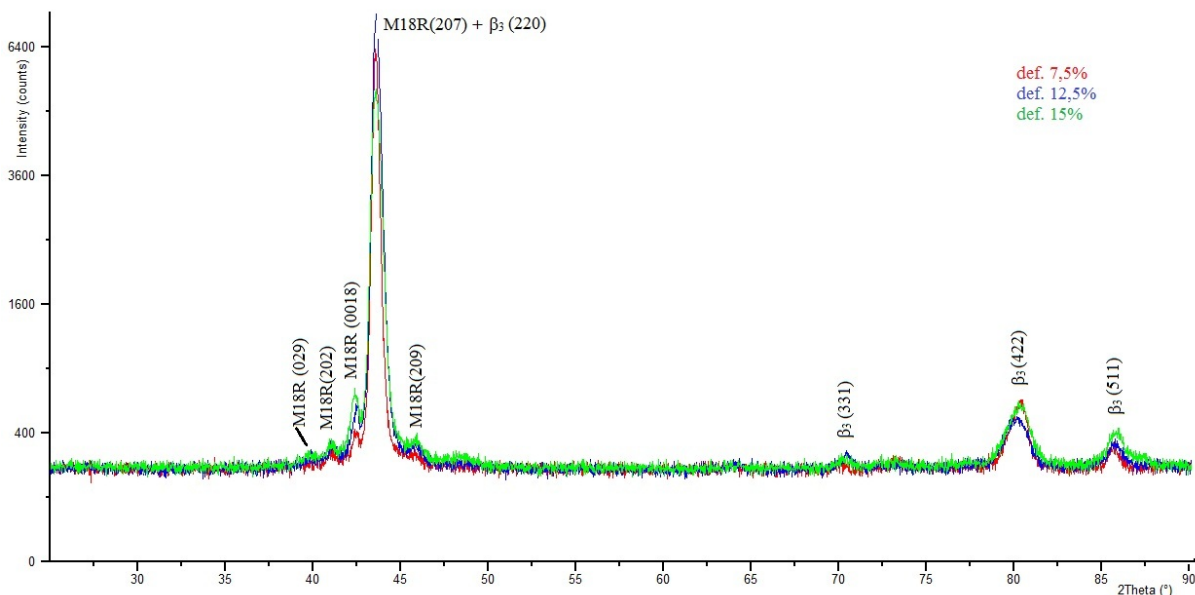


Figure 9: Comparison between the diffractograms of samples deformed up to 7.5%, 12.5% and 15%.





The rolling process was arrested at the deformation of 15%, in fact during the rolling deformation at 15% the samples have undergone a dramatic damage caused by the nucleation of many transgranular cracks (Fig. 10).

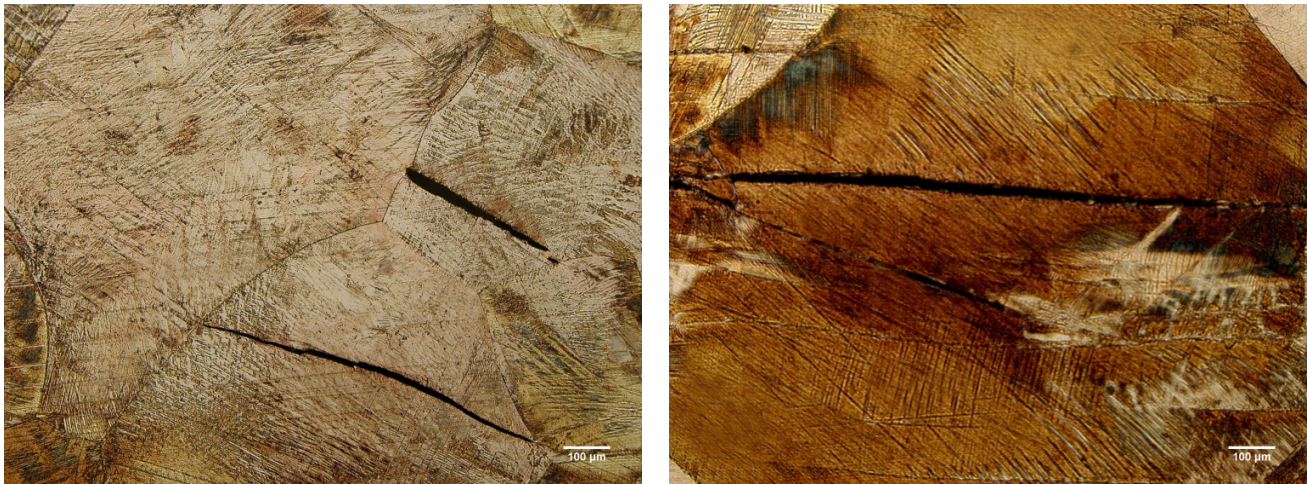


Figure 10: Transgranular cracks on the 15% deformed samples.

## CONCLUSIONS

The effects of the mechanical treatment of cold rolling of a Cu-Zn-Al, on which through a special heat treatment had been previously induced a  $L_{21}$  type order of the structure, have been investigated in this work. The deformation has contributed to  $\beta_3$  ( $L_{21}$ ) ordering of the structure and to generate the martensitic transformation. The martensite obtained is the M18R type. This result shows that the parameter which most influences the type of obtainable martensite is determined by the order of the parent phase. The martensite enucleates in appreciable quantities, as found during testing, already at a level of deformation of 2.5%. An increase of the martensite up to a deformation of 15% was observed. It has not been possible to continue beyond this level of deformation, due to the presence of transgranular cracks.

## REFERENCES

- [1] Daley L. Material Science and Technology (Phase Transformation in Material vol 5) ed. P.Haasen (1991).
- [2] R. Rapacioli, M. Ahlers, Scripta Met., 11 1(1977) 147.
- [3] M. H. Wu, J. Perkins, C. M. Wayman, Acta Met., 37 (1989) 1821.
- [4] M. Mantel, R. Rapacioli, G. Guerin, In: ICOMAT Nora, Japan Institute of Metals, Tokio, (1986) 880.
- [5] Y.S.Han, Y.G.Kim, J.Mater Sci., 21 (1986) 2711.
- [6] K.Otsuka, C.M. Wayman, K.Nakai, H.Sakamoto, K.Shimizu, Acta Metall., 24 (1976).
- [7] J.G. Boyd, D.C. Lagoudus, J.int Mater. Sys. Struct., 5 (1994) 333.
- [8] F. Lanzini, R. Romero, M. Stipcich, J. Phys.: Condens. Matter, 23 (2011) 405404,
- [9] R. Rapacioli, M. Ahlers, Scripta Metallurgica, 11 (1977) 1147.
- [10] S.C. Singh, Y. Murakami, L. Delaey, Scripta Metallurgica, 12 (1978) 435.
- [11] PowderCell 2.3-Pulverdiffraktogramme aus Einkristalldaten und Anpassung experimenteller Beugungsaufnahmen. [http://www.bam.de/de/service/publikationen/powder\\_cell.htm](http://www.bam.de/de/service/publikationen/powder_cell.htm).
- [12] N. Kayali, S. Bgen, O. Adiguzel, Materials Research Bulletin, 32(5) (1997) 565.
- [13] M. Zolliker, W. Bührer. Crystal Structure of Cu-Zn-Al Martensite. University Leuven.
- [14] Ken Gall, Huseyin Sehitoglu, Hans J. Maier, K. Jacobus, Metallurgical and Materials Transactions A, 29A (1998) 765.
- [15] K. Adachi, J. Perkins, Metallurgical Transactions A, 17A (1986) 945.